THE JOURNAL OF BIOLOGICAL CHEMISTRY Vol. 279, No. 42, Issue of October 15, pp. 44093–44100, 2004
Printed in U.S.A.

Mammary Gland Remodeling Depends on gp130 Signaling through Stat3 and MAPK*

Received for publication, December 2, 2003, and in revised form, July 26, 2004
Published, JBC Papers in Press, July 30, 2004, DOI 10.1074/jbc.M313131200

Ling Zhao‡§, Stefan Hart¶, JrGang Cheng‖, J. Joseph Melenhorst, Brian Bierie‡, Matthias Ernst‡‡, Colin Stewart‖, Fred Schaper§§, Peter C. Heinrich§§, Axel Ullrich¶, Gertraud W. Robinson‡, and Lothar Hennighausen‡¶ ¶¶**

*From the ‡Laboratory of Genetics and Physiology, NIDDK, National Institutes of Health, Bethesda, Maryland 20892, the ¶Max Planck Institute for Biochemistry, Martinsried 81399, Germany, the ‖Laboratory of Cancer and Developmental Biology, NCI, National Institutes of Health, Frederick, Maryland 21702, the **Hematology Branch, NHLBI, National Institutes of Health, Bethesda, Maryland 20892, the ‡‡Ludwig Institute for Cancer Research, Melbourne, Vic 3050, Australia, and the §§Department of Biochemistry, RWTH, Aachen 52074, Germany*

The interleukin-6 (IL6) family of cytokines signals through the common receptor subunit gp130, and subsequently activates Stat3, MAPK, and PI3K. Stat3 controls cell death and tissue remodeling in the mouse mammary gland during involution, which is partially induced by IL6 and LIF. However, it is not clear whether Stat3 activation is mediated solely through the gp130 pathway or also through other receptors. This question was explored in mice carrying two distinct mutations in the *gp130* gene; one that resulted in the complete ablation of gp130 and one that led to the loss of Stat3 binding sites (gp130Δ/Δ). Deletion of gp130 specifically from mammary epithelium resulted in a complete loss of Stat3 activity and resistance to tissue remodeling comparable to that seen in the absence of Stat3. A less profound delay of mammary tissue remodeling was observed in gp130Δ/Δ mice. Stat3 tyrosine and serine phosphorylation was still detected in these mice suggesting that Stat3 activation could be the result of gp130 interfacing with other receptors. Experiments in primary mammary epithelial cells and transfected COS-7 cells revealed a p44/42 MAPK and EGFR-dependent Stat3 activation. Moreover, the gp130-dependent EGFR activation was independent of EGF ligands, suggesting a cytoplasmic interaction and cross-talk between these two receptors. These experiments establish that two distinct Stat3 signaling pathways emanating from gp130 are utilized in mammary tissue.

gp130 is the common receptor subunit of IL6 family cytokines, which include interleukin-6 (IL6),[1] interleukin-11 (IL11), leukemia inhibitory factor (LIF), ciliary neurotrophic factor (CNF), oncostatin M (OSM), cardiotrophin-1 (CT-1), interleukin-27 (IL27), neuropoietin (NP), and cardiotropin-like cytokine (CLC) (1–6). This receptor subunit is expressed ubiquitously and mediates a variety of biological functions. Targeted disruption of the *gp130* gene in mice causes thinning of ventricular myocardium, reduction of hematopoietic stem cells and structural and functional defects in the placenta, which results in embryonic lethality (7). gp130 is also involved in orchestrating immune responses, hematopoietic development, host response to infectious and inflammatory stimuli, cell-cell communication, and cell cycle regulation (8–10).

In the mammary gland, the cycle of development and function includes the proliferation of alveolar epithelium during pregnancy, differentiation with parturition, and cell death and remodeling upon weaning of the young (11). Two key events have been linked to the initiation of cell death and tissue remodeling during involution. First, the induction of milk stasis, which results in the up-regulation of *IL6* (12) and *LIF* (12, 13) gene expression, and the activation of the transcription factor Stat3 (14). While loss of Stat3 resulted in severe retardation of mammary epithelial cell death and impaired remodeling (15, 16), less severe lesions were observed in IL6- (12) and LIF-null (12, 17) mice.

Stat3 can be activated by several cytokines, which signal through distinct receptors, including receptor-tyrosine kinases (RTK), single-chain cytokine receptors, and receptors that share the common subunit gp130. While IL6 family cytokine-induced Stat3 activation is dependent on gp130 and Janus kinases (Jak), Jak-independent activation can be accomplished through the EGFR that possesses an endogenous tyrosine kinase and the ability to activate several other intracellular tyrosine kinases (18, 19).

Since IL6 and LIF are key inducers of Stat3 phosphorylation in mammary tissue at the onset of involution it was necessary to explore the possibility that the key signaling events are mediated by their common receptor gp130. Toward this end, two mouse mutants were employed. In one mouse model, the entire *gp130* gene was inactivated in mammary epithelium using Cre-loxP-mediated recombination. In the other model, a truncated mutation of the C terminus of gp130 (gp130Δ/Δ) was introduced as the Y765F, Q768A, and 769stop substitutions (20). This resulted in the loss of the four Stat3 binding sites ($Tyr^{765,812,904,914}$). However, the SHP2 and Jak2 binding sites were intact, and therefore the emanating signals were functional in this mutant. The physiological lesions imposed by the loss of Stat3 signaling through the gp130Δ/Δ receptor (20) mimicked those observed in the absence of IL6 (21) or LIF (22). Since the MAPK pathway was unimpeded in these mice we

* The costs of publication of this article were defrayed in part by the payment of page charges. This article must therefore be hereby marked "*advertisement*" in accordance with 18 U.S.C. Section 1734 solely to indicate this fact.

§ Current address: Genetics and Molecular Biology Branch, National Human Genome Research Institute, Bethesda, MD 20892.

¶¶ To whom correspondence should be addressed: Laboratory of Genetics and Physiology, NIDDK, National Institutes of Health, Bethesda, MD 20892. E-mail: hennighausen@nih.gov.

[1] The abbreviations used are: IL6, interleukin-6; EGFR, epidermal growth factor receptor; MAPK, mitogen-activated protein kinase; JAK, Janus kinase; DMEM, Dulbecco's modified Eagle's medium; Stat, signal transducers and activators of transcription; LIF, leukemia inhibitory factor; OSM, oncostatin M; wt, wild type.

were able to also explore its contribution to tissue remodeling in involuting mammary epithelium.

EXPERIMENTAL PROCEDURES

Animals—All animals used in the course of this study were treated within published guidelines of humane animal care.

Inactivation of the gp130 Gene in Mouse Mammary Epithelium—Mice were generated in which loxP sites were inserted into the promoter and intron II,[2] which made it possible to specifically delete exons I and II (gp130 fl/fl). A transgene encoding Cre recombinase under the control of the *WAP* gene promoter (23, 24) was bred into gp130 fl/fl mice to achieve recombination in mammary epithelium. These mice are referred to as gp130 fl/fl;WC throughout the text.

Transplantation of Mammary Epithelium—LIF−/− (22), wild type (wt), gp130Δ/Δ (20), gp130 fl/fl,[2] gp130 fl/fl;WC, Stat3 fl/fl;WC and Stat3 fl/fl (25) mice were used as donors. 3-week-old athymic nu/nu mice (DCT, Frederick, MD) were used as recipients. All mice were anesthetized using Avertin (200 μl/10 g BW) prior to surgery. The proximal part of the number four glands (both left and right) containing the epithelium of all recipient mice were excised, and the donor mammary tissue (1 mm^3) was transplanted into the cleared fat pad. Eight weeks after transplantation, the nude mice were mated, and pups were removed at birth. The number 3 endogenous gland and both transplanted glands were harvested on the day of birth of pups (L1) and days 1 (i1), 2 (i2), 3(i3), 4 (i4), and 6 (i6) of involution.

E12.5 day embryo mammary anlagen from Jak2-null and wt embryos were transplanted to nude mice as described before (26). The transplanted mammary tissue was allowed to grow for 8 weeks before harvest.

Histology and Immunohistochemistry/Immunofluorescence—Tissues were fixed in 10% neutral buffered formalin overnight at 4 °C, dehydrated, and embedded in paraffin. Tissue blocks were sectioned at 5 μm and stained with hematoxylin and eosin. For immunostaining, tissue sections on poly-L-lysine-coated slides were deparaffinized in xylene and rehydrated in decreasing ethanol concentrations. All tissue sections were treated with antigen unmasking reagent (Vector Laboratories) by boiling for 10 min following the manufacturer's protocol. The Stat5a antibody (14) was used at a 1:600 dilution. The Stat3 antibody (Santa Cruz Biotechnology) was diluted 1:200. Antibodies for gp130 (Santa Cruz Biotechnology), β-catenin (Transduction Laboratories) and Npt2b (a gift from Dr. Jürg Biber, Department of Physiology, University of Zürich, Zürich, Switzerland) (27) were used at a 1:100 dilution. All primary antibodies were incubated with sections overnight at 4 °C. Immunoperoxidase staining was performed according to the manufacturer's protocol (Vector ABC kit, DAB substrate kit, Vector Laboratories). For immunofluorescence, Alexafluor-conjugated secondary antibodies (Molecular Probes) were incubated with sections for 30 min at room temperature in the dark, then mounted in Vectashield (Vector Laboratories) and visualized with a microscope (Olympus) using a mercury bulb for excitation of the fluorescent conjugates.

Western Blots—Protein was extracted from frozen tissues (1 g/10 ml lysis buffer), homogenized in lysis buffer (10 mM Tris-HCl, pH 8.0; 5 mM EDTA; 50 mM NaCl; 30 mM $Na_4P_2O_7$; 50 mM NaF; 200 μM Na_3VO_4; 1% Triton-X 100; 1 mM phenylmethylsulfonyl fluoride; 5 μg/ml aprotinin; 1 μg/ml pepstatin A, and 2 μg/ml leupeptin) using a Polytron. The homogenate was incubated on a vertical rotator at 4 °C for 1 h, and fat was cleared from extracts by spinning twice at 14,000 rpm at 4 °C for 20 min. 100 μg of protein from each sample was fractionated in 8 and 14% Tris-glycine gels (Invitrogen) and transferred onto polyvinylidene difluoride (Invitrogen) membrane using a Novex Western blot apparatus. After transfer and blocking (5% bovine serum albumin and 2% nonfat milk, 20 mM Tris-HCl, pH 7.6/137 mM NaCl) at room temperature for 1 h, the membranes were incubated with primary antibodies (1:1000 diluted) as follows. Stat5a (14), WAP (28), Stat3, gp130, Stat1, Bax, SGP2, EGFR (Santa Cruz Biotechnology), P-Stat3-Tyr (705), P-Stat3-Ser (727), Stat3, P-p44/42 (Thr^{202}/Tyr^{204}) MAPK, p44/42 MAPK, P-p38 (Thr^{180}/Tyr^{182}) MAPK, p38 MAPK, P-Akt (Ser^{473}), Akt (Cell Signaling), and actin (1:4000, Chemicon). All primary antibodies were applied for 1 h at room temperature or at 4 °C overnight. The membranes were incubated with secondary horseradish peroxidase-conjugated antibodies (Transduction Laboratories, 1:5000) for 30 min at room temperature. Proteins were visualized using the ECL detection system (Amersham Biosciences). Blots were stripped using a Western stripping buffer (Alpha Diagnostic) for 20 min at room temperature.

Involution Experiments—At day 10 of lactation, pups were removed from both gp130-null and wild-type mice. The number 4 gland from the left side was collected by biopsy. Mice were sacrificed at days 1, 2, 3 of involution. Two weeks after weaning the right number 4 glands were collected for protein and histological analyses. The litter sizes were 7–10 pups. Three mice were used for each time point.

Cell Culture and Transfection—Primary mammary epithelial cells were obtained from wild type, gp130Δ/Δ and Jak2-null transplanted mammary tissues from 3–6 virgin mice. The mammary transplants were cut into fine pieces and subjected to collagenase III (2 mg/ml, Invitrogen) digestion at 37 °C for an hour. The digested tissues were put through 20-gauge needles and centrifuged at 1000 rpm for 3 min. The cell pellets were washed once with Dulbecco's modified Eagle's medium (DMEM, Invitrogen) supplemented with 10% fetal bovine serum. Subsequently mammary tissue (normally 3–5 cells in a cluster) was suspended in complete DMEM with insulin (10 μg/ml) and EGF (10 ng/ml), and seeded into 6-well tissue culture plates. Cells were left undisturbed for a week. The medium was changed to serum-free DMEM for 24 h, and the cells were treated with IL6 (10 ng/ml, 100 ng/ml, PeproTech), IL6 with U0126 (10 μM, Biomol), and AG1478 (3 μM, Biomol) for 15 min before harvesting for protein extraction. Cells were lysed using the lysis buffer described previously, and immunoprecipitation and Western blot were performed using standard procedures.

COS-7 cells were cultured in DMEM supplemented with 10% fetal bovine serum. Transfections of COS-7 cells with cDNA expression vectors (1.0 μg each) encoding wt gp130 (wt), gp130YYFFFF (YY are tyrosine residues 767, 814, 905, and 915 (which correspond to the tyrosine residues 765, 812, 904, and 914 in murine gp130, Ref. 29) were mutated to phenylalanine residues), IL6R (gp80) and control empty vector (EV) were carried out using LipofectAMINE (Invitrogen) according to the manufacturer's protocol. Briefly, for transient transfections in 6-cm dishes the cells were incubated for 24 h with the transfection mix containing 15 μl of Polyfect and 2 μg of total plasmid DNA per dish. Cells were washed and cultured in serum-free medium for another 24 h prior to IL6 stimulation. Cells were lysed for 10 min on ice in 200 μl of lysis buffer containing 50 mM HEPES, pH 7.5, 150 mM NaCl, 1% Triton X-100, 1 mM EDTA, 10% glycerol, 10 mM $Na_4P_2O_7$, 2 mM Na_3VO_4, 10 mM NaF, 1 mM phenylmethylsulfonyl fluoride, and 10 μg/ml aprotinin (HNTG). Lysates were precleared by centrifugation at 13,000 rpm for 10 min at 4 °C. 100 μl of lysates were immunoprecipitated using EGFR antibodies (108.1) (30) and 20 μl of protein A-Sepharose (Sigma) for 4 h at 4 °C. Precipitates were washed three times with 0.5 ml of lysis buffer, suspended in 2× SDS sample buffer, boiled for 3 min, and subjected to gel electrophoresis and Western blotting as described above. Phosphotyrosine was detected using the 4G10 monoclonal antibody (Upstate). Polyclonal anti-phospho-p44/p42 (Thr^{202}/Tyr^{204}) MAPK antibody, anti-phospho-Stat3, and Stat3 antibodies were purchased from New England Biolabs (Beverly, MA). Polyclonal anti-p44/42 MAPK antibody was from Santa Cruz Biotechnology.

Statistics—Western blot bands were quantified using Alpha image 2000 v4 software. Three independent experiments were used to quantitate the data for analysis. All bands were normalized to actin or unphosphorylated total protein. Data are shown as mean ± S.E., and a Student's *t* test was used to compare two groups of samples.

RESULTS

LIF Contributes to Mammary Epithelial Cell Death during Involution but Does Not Influence Mammary Development—The level of LIF expression increases sharply at the onset of involution (12), and its role in mammary epithelial cell death and tissue remodeling was therefore investigated. Since LIF-null mice are infertile, mammary tissue was transplanted into wild-type hosts and analyzed after puberty, during pregnancy and involution. In virgin mice, no histological differences were detected between wild type (Fig. 1*A*, *panel a*) and LIF-null (Fig. 1*A*, *panel d*) mammary tissue 8 weeks after transplantation. A ductal tree filled the entire fat pad and exhibited extensive branching. Analysis of *bona fide* LIF-null mice during puberty revealed an abnormal branching (Fig. 1*A*, *panels b* and *e*), and the effect was abolished upon transplantation (Fig. 1*A*, *panels a* and *d*). Moreover, similar morphology was observed during pregnancy in wild type and null transplanted tissue (Fig. 1*A*, *panels c* and *f*). This suggests that the lesion resulted from systemic or stromal effects in LIF-null mice.

To explore the contribution of LIF in the remodeling process, tissue was analyzed at parturition and days 1–6 of involution.

[2] J. Cheng and C. Stewart, unpublished data.

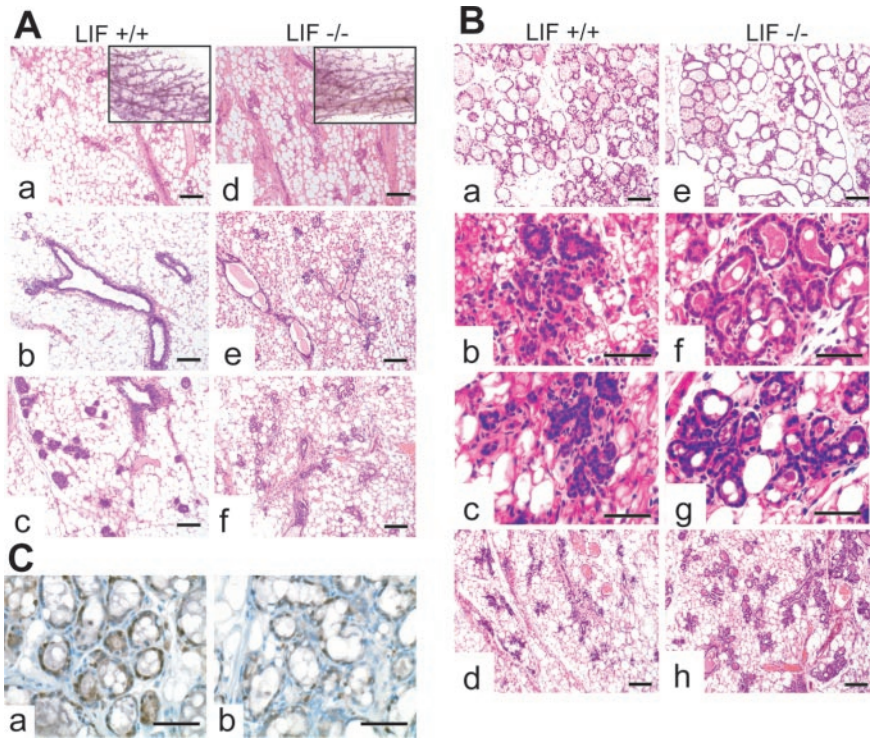

FIG. 1. **Histology of LIF−/− and +/+ mammary tissue at virgin, pregnancy, and involution stages.** *A*, virgin tissue from transplanted (*panels a* and *d*) and intact (*panels b* and *e*) animals. Whole mounts of transplanted glands are offset in the hematoxylin and eosin-stained images (*panels a* and *d*). *Panels c* and *f* are mammary tissues from day 13 pregnant wt (*c*) and LIF-null (*f*) mice. *Bar*, 50 μm. *B*, tissues harvested at L1 (*panels a* and *e*), day 3 (*i3-b*, *f*), day 4 (*i4-c*, *g*), and day 6 (*i6-d*, *h*) of involution from wt (*panels a–d*) and LIF-null (*panels e–h*) transplants. Bar, 50 μm. *C*, immunostaining of Stat3 (*panels a* and *b*) in LIF+/+ (*panel a*) and LIF−/− (*panel b*) mammary tissues at day 2 of involution.

No obvious differences were noted at parturition (Fig. 1*B*, *panels a* and *e*) and days 1 and 2 of involution (data not shown). However, from day 3–6 LIF-null tissue (Fig. 1*B*, *panels f–h*) retained more alveoli, and the reappearance of the stroma was delayed. Histological differences between LIF-null and wild-type mammary tissues were observed until day 6 of involution (Fig. 1*B*, *panels d* and *h*). Less nuclear Stat3 staining was observed in LIF-null tissue (Fig. 1*C*).

In addition to LIF and IL6, expression of OSM, another IL6 family cytokine, was also detected in mammary tissue. OSM expression in involuting glands peaked at 24 h and was absent in lactating glands (data not shown). This suggests that OSM may also be involved in mammary tissue remodeling.

Inactivation of the gp130 Gene in Mammary Epithelium—To examine the contribution of the receptor subunit gp130 in the remodeling of mammary epithelium and in the activation of Stat3, we analyzed mice with two distinct mutations in the *gp130* gene. One strain expressed a gp130 with a truncated C-terminal region, and in the other strain the entire gene was inactivated.

Deletion of Stat3 Binding Sites in gp130—The *gp130* gene in gp130Δ/Δ mice carries a knockin mutation (20) that results in a C-terminal truncation at amino acid 769 and a loss of all proposed Stat3 binding sites (31). Since these mice are infertile mammary tissue was transplanted into wild-type recipients, and the ability of the cells to develop during pregnancy and subsequently engage in remodeling was examined. While pregnancy-induced mammary development was normal (data not shown), involution was delayed (Fig. 2*A*). Wild-type tissue at day 3 of involution had undergone extensive remodeling (Fig. 2*A*, *panel b*) but mutant mammary tissue continued to display distended alveoli with evidence of milk secretion (Fig. 2*A*, *panel e*). The levels of milk protein WAP and apoptosis-related protein SGP2 also confirmed the delayed involution (Fig. 2*B*). However, this delay of remodeling was transient and full involution was eventually achieved. The levels of Stat3 and MAPK activation in gp130Δ/Δ tissue was examined by Western blot analyses (Fig. 2*B*). Phosphorylated Stat3 was still present in mutant tissue, while phosphorylated p44/42 MAPK appeared to be lower (Fig. 2*B*). This suggests that Stat3 can be activated in mammary tissue through pathways that are independent of the known Stat3 binding sites in gp130. This possibly occurs through activation by the LIFR, which dimerizes with gp130Δ/Δ.

Complete Inactivation of gp130—The gp130Δ/Δ mutation resulted in the loss of Stat3 binding sites but retained the SHP2 and Jak2 binding sites, and therefore intact MAPK signaling, which contributes to the involution process (12). To fully understand the gp130-activated signals in mammary tissue remodeling it was therefore necessary to inactivate the entire protein. Mice were generated that carried loxP sites in the promoter of the *gp130* gene and in intron II.[2] This permitted the complete inactivation of the gene through Cre-mediated recombination. The *gp130* gene was specifically inactivated in differentiating mammary epithelium during pregnancy using the WAP-Cre transgene (23, 24). Mammary tissue was analyzed from gp130 fl/fl;WC mice after one and several pregnancies by Western blots and histology analysis. Greatly reduced levels of gp130 were observed in gp130 fl/fl;WC mice ($p < 0.05$) (Fig. 3*A*). The residual signal was due to the stromal compartment of the gland in which the WAP-Cre transgene is not active. The levels of phosphorylated p44/42 MAPK were lower after two pregnancies, and after five pregnancies both the total amount and phosphorylated form of p44/42 MAPK were reduced (Fig. 3*A*, $p < 0.05$) compared with fl/fl mice.

Cre activity in WAP-Cre transgenic mice is activated strongly during the first pregnancy and leads to gene deletion such that all cells in subsequent pregnancies derive from progenitor cells in which recombination occurred (24). In order to obtain extensive inactivation of the *gp130* gene, gp130 fl/fl;WC mice were taken through two pregnancies, followed by the analysis of mammary tissue during involution. In these mice involution and the associated tissue remodeling was greatly impaired (Fig. 3*B*), and the glands had a secretory appearance even 2 weeks after weaning (Fig. 3*C*, *panels b* and *d*). Immunofluorescence confirmed the absence of gp130 in gp130 fl/fl;WC (Fig. 4*A*) tissue and its presence in fl/fl (Fig. 4*D*) mammary tissue. The sodium phosphate transporter Npt2b at the

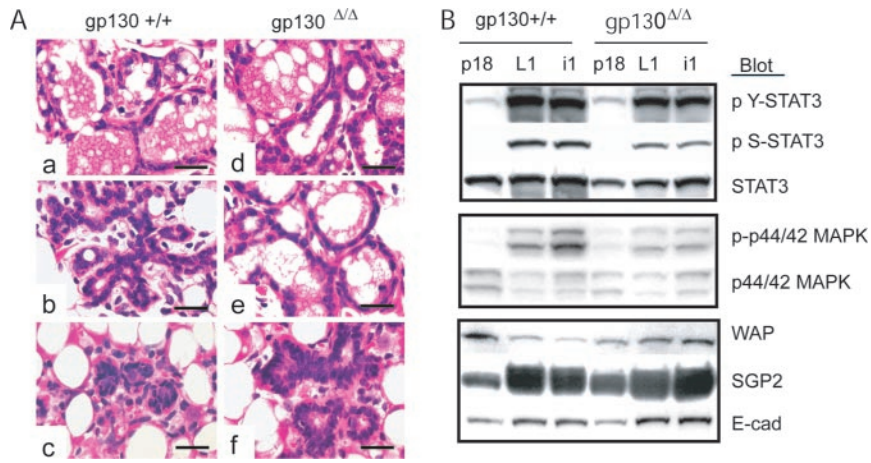

FIG. 2. *A*, histology of mammary transplants from wt (*panels a–c*) and gp130Δ/Δ (*panels d–f*) mammary tissues at day 1 (*i1-a*, *d*), day 3 (*i3-b*, *e*), and day 4 (*i4-c*, *f*) of involution. *Bar*, 50 μm. *B*, Western blot of p-Stat3, Stat3, p-p44/42 MAPK, p44/42 MAPK, WAP, SGP2, and E-cadherin from wt and gp130Δ/Δ mammary tissues at day 18 of pregnancy (*p18*), at parturition (*L1*), and day 1 of involution (*i1*). p18 serves as a control for the non-involuting gland because at L1, the transplanted tissue has started to involute.

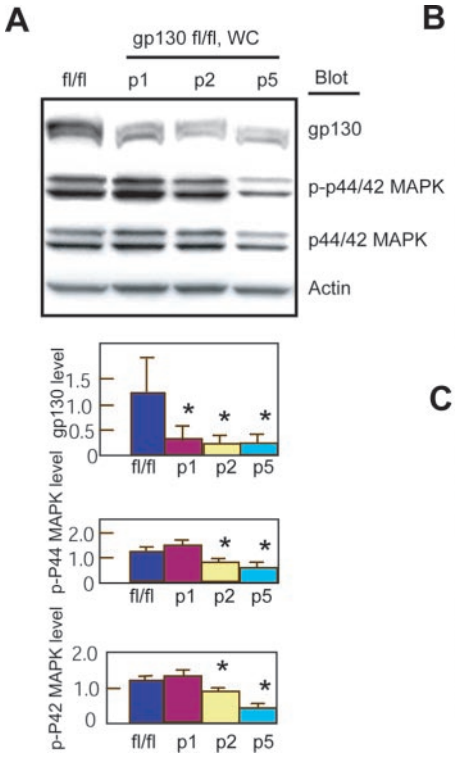

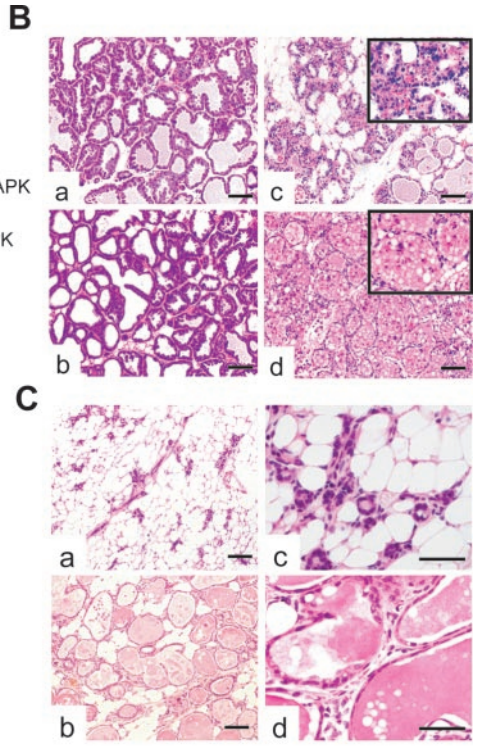

FIG. 3. *A*, Western blot analysis of gp130 protein after 1 (*P1*), 2 (*P2*), and 5 (*P5*) pregnancies in gp130 fl/fl (*fl/fl*) and gp130 fl/fl;WC (*fl/fl;WC*) mammary tissues. The level of gp130 protein is lower in all fl/fl;WC samples compared with fl/fl tissue ($p < 0.05$). p-p44/42 MAPK level is also lower after two pregnancies in fl/fl;WC tissue compared with that of the fl/fl tissue. *, $p < 0.05$. *B*, histology of L10 (*panels a* and *b*) and day 3 involution mammary glands (*panels c* and *d*) from gp130 fl/fl (*panels a* and *c*) and gp130 fl/fl;WC (*panels b* and *d*) mice. Enlarged images are embedded in *panels c* and *d*. *Bar*, 100 μm. *C*, morphology of mammary glands harvested 2 weeks after weaning from fl/fl (*panels a* and *c*) and fl/fl;WC (*panels b* and *d*) mice. *Bar*, 100 μm (*panels a* and *b*) and 50 μm (*panels c* and *d*).

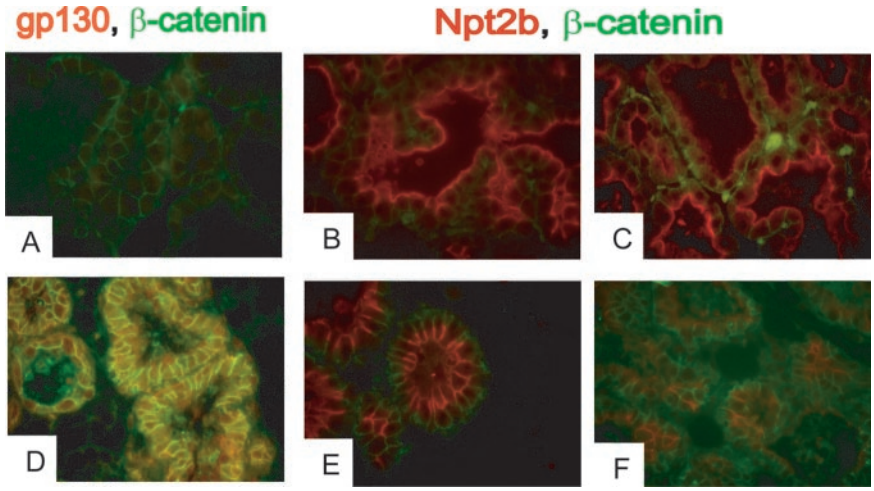

FIG. 4. **Immunofluorescence of gp130 (*A* and *D*; *red*), Npt2b (*B*, *C*, *E*, and *F*; *red*) and β-catenin (*A–F*; *green*) in gp130 fl/fl;WC (*A–C*) and gp130 fl/fl (*D–F*) tissues at L10 (*B* and *E*) and day 2 (*i2*) of involution (*A*, *C*, *D*, *F*).** The gp130 signal was absent in gp130 fl/fl;WC tissue (*A*) but appeared in fl/fl tissue (*D*). Npt2b staining was similar in L10 (*B*, *E*) tissues but remained at a high level in gp130 fl/fl; WC tissue (*C*), while it had declined in the fl/fl tissue (*F*).

apical membrane of mammary alveolar epithelium, which reflects its functional status (32), was present in mammary epithelium from gp130 fl/fl; WC mice 2 days after weaning (Fig. 4*C*), similar to that seen in tissue from wild-type lactating mice (Fig. 4*E*). In contrast, greatly reduced levels were observed in the tissue from gp130 fl/fl mice at day 2 of involution (Fig. 4*F*).

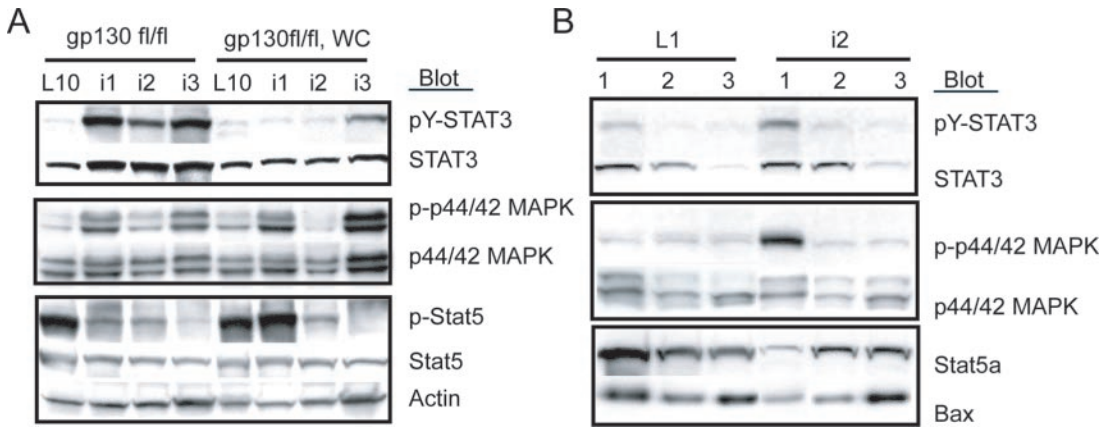

FIG. 5. *A*, Western blot analyses of Stat3, p44/42 MAPK, and Stat5 activation in mammary tissues from gp130 fl/fl and gp130 fl/fl;WC mice at day 10 of lactation (L10), day 1(*i1*), 2 (*i2*) and 3 (*i3*) of involution. Stat3 activation was absent in the fl/fl;WC tissues from i1 and i2 but started to increase on i3. *B*, Western analysis of Stat3, Stat5, and p44/42 MAPK at the day of birth (*L1*) and day 2 of involution (*i2*) from transplanted mammary tissues of gp130 fl/fl;WC and Stat3 fl/fl;WC mice. *Lane 1*, endogenous glands; *lane 2*, gp130 fl/fl;WC; *lane 3*, Stat3 fl/fl;WC. P-Stat3 and p-p44/42 MAPK levels are low in gp130 and Stat3-null (*lanes 2* and *3*) tissues.

This, again, established that the normal involution process was not executed in gp130-deficient mammary epithelium.

Upon loss of gp130, no induction of Stat3 phosphorylation was observed in mammary tissue during involution (Fig. 5*A*). In contrast, Stat3 tyrosine phosphorylation was rapidly induced upon weaning in wild-type mammary tissue (14) (Fig. 5*A*). The higher levels of pY-Stat3 3 days after weaning could be the result of parallel pathways, which however, are not sufficient to induce involution. P-p44/42 MAPK was present in gp130-null epithelium suggesting that this pathway can be activated by receptors other than gp130. The loss of Stat5 phosphorylation, and thereby loss of transcriptional activity, is a hallmark of the early steps of involution, which are characterized by a loss of differentiation (14). The decline of phosphorylated Stat5 was delayed in gp130-null tissue as compared with wild-type tissue (Fig. 5*A*) supporting the notion that gp130-null tissue retains its function.

If Stat3-induced tissue remodeling is solely controlled through the gp130 pathway, loss of either signaling component should lead to identical consequences. In order to examine the differences between the gp130- and Stat3-null mammary tissue, a side-by-side comparison of gp130-null and Stat3-null mammary tissue from contralateral transplants were performed. The results revealed that the delay in tissue remodeling was histologically indistinguishable between these two mutants (Fig. 6). Stat3 activation was severely impaired upon inactivation of the *gp130* gene and absent in Stat3-null mammary tissue (Fig. 5*B*). Moreover, p44/42 MAPK phosphorylation was reduced in mammary tissue lacking either gp130 or Stat3 (Fig. 5*B*). The levels of the cell death protein Bax increased in Stat3-null but not in gp130-null tissues (Fig. 5*B*), suggesting that Stat3-independent components of gp130 signaling control its expression.

*gp130*Δ/Δ *Signaling Leads to Stat3 Phosphorylation and EGFR Activation*—Although the gp130Δ/Δ had lost its Stat3 binding sites, both tyrosine and serine phosphorylation of Stat3 were detected in mammary tissue from the mutant mice (Fig. 2*B*), and in primary mammary epithelial cells from gp130Δ/Δ transplants (Fig. 7*A*). This suggested that receptors other than gp130 contributed to Stat3 activation in mammary epithelium. Since absence of the entire gp130 resulted in the complete loss of Stat3 phosphorylation, we hypothesized that the C-terminal region of gp130Δ/Δ, which contains binding sites for the tyrosine kinases Jak1, Jak2, and Tyk2 and for SHP2, was capable of activating Stat3. For example, Stat3 activation through the LIFR could be achieved through the Stat3 binding site in the receptor α-chain that dimerizes with gp130Δ/Δ, a scenario that is not feasible for IL6.

To evaluate whether Jak2 controlled Stat3 and MAPK activity, Jak2-null mammary epithelial cells from transplanted tissue were analyzed. The absence of Jak2 in mammary epithelium did not adversely affect IL6-induced Stat3 activation (Fig. 7*A*) or MAPK phosphorylation (Fig. 7*B*). Stat3 activation can also be accomplished through the EGFR and the possibility that IL6 can induce Stat3 through the EGFR was tested. In primary mammary epithelial cells from wild type and gp130Δ/Δ transplants, basal levels of EGFR phosphorylation were detected, which in wild-type cells were enhanced by IL6 (Fig. 7*C*). The basal level of EGFR phosphorylation might be attributed to the EGF in the culture medium, even though the cells were changed to serum-free medium for 24 h prior to the experiment. As the p44/42 MAPK phosphorylation level was lower in gp130Δ/Δ tissue than in wild-type tissue (Fig. 2*B*), the possibility existed that activation of the upstream phosphatase SHP2 was impaired. Its activation was examined, and SHP2 phosphorylation was detected in gp130Δ/Δ tissue as well as in wild-type tissue, both in the absence and presence of IL6 (Fig. 7*C*).

p44/42 MAPK and the EGFR Contribute to Stat3 Activation—Loss of Stat3 binding sites in gp130 corresponded to lower levels of p44/42 MAPK phosphorylation, thus suggesting a link between these two signaling components. To explore this further, primary mammary epithelial cells from wild-type, gp130Δ/Δ, and Jak2-null mice were treated with MAPK (U0126) and EGFR (AG1478) inhibitors. Phosphorylation of p44/42 MAPK was abolished by U0126 and decreased by AG1478 treatment (Fig. 7*B*) in all cells examined. Total p44/42 MAPK levels were lower (Fig. 7*B*), and Stat3 tyrosine and serine phosphorylation were reduced (Fig. 7*A*) upon treatment with these inhibitors. Stat3 can be phosphorylated by the EGFR (33–35), and the EGFR itself can be activated by other receptors through a process called transactivation. In this process, receptors such as those coupled to G proteins, activate proteases, which subsequently release EGF-type ligands (36). We therefore asked whether gp130 was capable of activating the EGFR in a similar manner. IL6 elicited very little EGFR phosphorylation in COS-7 cells (Fig. 7*D*). However, IL6 induced EGFR phosphorylation in the presence of exogenous IL6R (Fig. 7*D*, *gp80*) and wild-type gp130 (Fig. 7*D*, *wt*). EGFR activation was also observed in the presence of a gp130 receptor in which all four Stat3 binding sites had been mutated (YY). This indicates that the truncated gp130 can transduce signals upon IL6

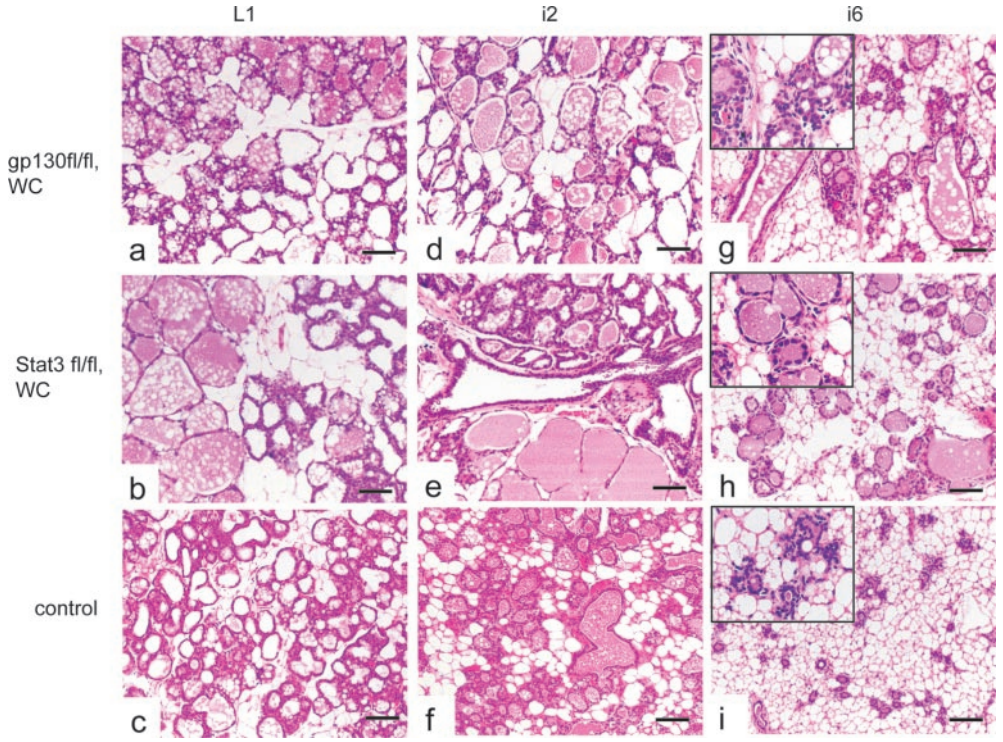

FIG. 6. **Histology of mammary tissues from endogenous control (*panels c, f, i*), transplanted gp130 fl/fl;WC (*panels a, d, g*) and Stat3 fl/fl;WC (*panels b, e, h*) at the day of birth (*L1-a, b, c*), day 2 (*i2-d, e, f*) and 6 (*i6-g, h, i*) of involution.** The surgical procedure separates the nipple from the transplanted tissue, pups could not suckle the gp130 fl/fl;WC (*panels a, d, g*) and Stat3 fl/fl;WC (*panels b, e, h*) glands. Therefore, these two glands will start involution earlier than the endogenous gland. *Enlarged pictures* are embedded in *panels g*, *h*, and *i*. *Bar*, 100 μm.

stimulation, which result in EGFR phosphorylation. Moreover, Stat3 activation was observed both in the presence of a wild-type gp130 molecule and the mutated gp130 without functional Stat3 binding sites (Fig. 7*D*). A slight activation of p42 MAPK was observed in the presence of the IL6R and gp130.

In the classical transactivation process metalloproteases from the ADAM family cleave transmembrane EGF-like ligand precursors and the released ligands subsequently activate the EGFR. To further explore whether IL6 can activate the EGFR and thereby Stat3 through such a process, we made use of two distinct inhibitors, the diphtheria toxin mutant CRM197, which inhibits proHB-EGF, and the anti-EGFR antibody ICR-3R, which blocks the binding of ligands. Pretreatment with the CRM197 did not block EGFR tyrosine phosphorylation in response to IL-6 stimulation of COS-7 cells transfected with the *GP80/YY* mutant (Fig. 8). Furthermore, pretreatment of the cells with the monoclonal anti-EGFR antibody ICR-3R for 60 min blocked direct stimulation of the EGFR with EGF, but did not interfere with IL-6-induced EGFR tyrosine phosphorylation (Fig. 8). This strongly suggests an EGFR ligand-independent cross-talk between the gp130 mutant YY and the EGFR.

DISCUSSION

The death of mammary epithelium in conjunction with tissue remodeling is the hallmark of mammary gland involution after weaning and is required for the successful rebuilding of the gland during the following pregnancy. Stat3 has been identified as a key regulator of involution-associated epithelial cell death and tissue restructuring (15, 16) and the specific mediators leading to its activation are now emerging. Both IL6 (12, 17) and LIF (12, 17) contribute to the induction of mammary tissue remodeling through their respective receptors and the activation of Stat3. Loss of either cytokine alone results in a delayed onset of involution but tissue remodeling is eventually accomplished. At this point it is not clear whether additional members of the IL6 family contribute to the remodeling process through the activation of Stat3. The expression pattern of OSM during mammary involution (data not shown) mimics that of IL6 suggesting also a similar role for this cytokine. Although LIF partially controls mammary gland remodeling through the activation of Stat3, this study demonstrates that its absence during puberty and pregnancy does not adversely affect normal ductal elongation and branching as well as alveolar development during pregnancy. These findings are in contrast to a study by Kritikou *et al.* (17) who reported precocious mammary development during pregnancy in LIF-null mice. The nature of the discrepancy is unknown.

This study provides compelling evidence that LIF and IL6 signal through the gp130 receptor using both a traditional and an unconventional signaling route. Inactivation of the entire *gp130* gene in mouse mammary epithelium resulted in a complete loss of Stat3 phosphorylation and in developmental consequences that are congruent with those seen in Stat3-null mice, namely a delay of tissue remodeling. This demonstrates that Stat3 activation prior to mammary epithelial cell death and tissue remodeling is initiated through gp130 signaling. However, Jak-mediated phosphorylation of Stat3 not only occurs through the classical Stat3 binding sites in the C terminus of gp130, but also through a mechanism dependent on other pathways emanating from gp130. Specifically, Stat3 phosphorylation was observed in mice that carried the truncated mutant gp130Δ/Δ. This mutant lacks all Stat3 binding sites but retains the Jak1, Jak2, Tyk2, and SHP2 recruitment sites (20), and therefore contains intact MAPK and PI3K signal pathways, which may contribute to the activation of Stat3.

Our study demonstrates that gp130-dependent Stat3 phosphorylation does not require the Stat3 docking sites on gp130, but needs only the highly conserved box1–2 region, recognized by Jak1, Jak2, and Tyk2. MAPK and EGFR inhibitors greatly suppressed serine phosphorylation of Stat3, which was almost abolished after the combined treatment with these two inhib-

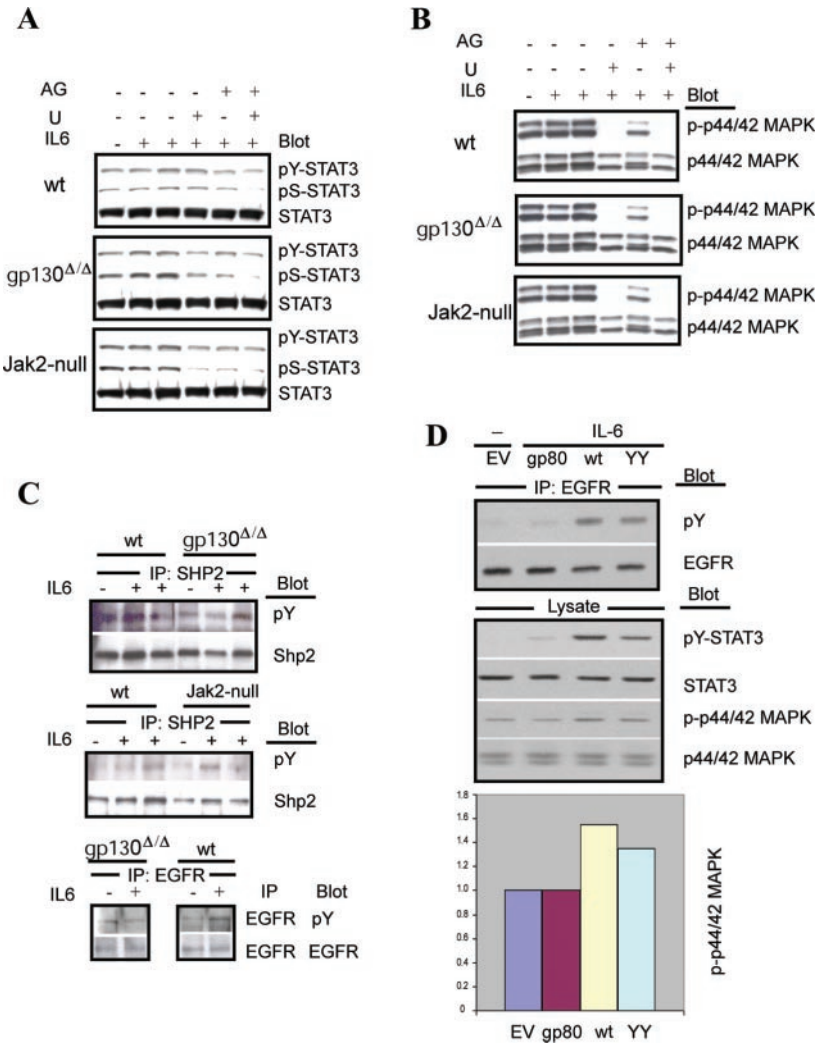

FIG. 7. *A*, Stat3 activation in wt, gp130Δ/Δ and Jak2-null mammary epithelial cells. Cells were treated with IL6 (10 ng/ml and 100 ng/ml-*lane 3 only*), MAPK inhibitor (U0126) and EGFR inhibitor (AG1478) for 15 min. Stat3 tyrosine and serine phosphorylation were reduced upon treatment with both U0126 and AG1478. *B*, p44/42 MAPK activation in wt, gp130Δ/Δ, and Jak2-null mammary epithelial cells. Cells were treated as described above. p44/42 MAPK activation were abolished by the use of U0126, and decreased by AG1478. *C*, phosphorylation of SHP2 and EGFR in mammary cells of wt, gp130Δ/Δ, and Jak2-null without IL6 treatment. *D*, endogenous EGFR tyrosine phosphorylation, p44/42 MAPK and Stat3 phosphorylation in response to IL6 stimulation. COS-7 cells were transiently transfected with cDNAs encoding gp80-IL6R (*gp80*), gp130wt (*wt*), with gp80, gp130YYFFFF (*YY*) (the Stat3 binding sites $Tyr^{767,814,905,915}$ had been mutated to phenylalanine residues, but the SHP2 binding sites had remained intact) with gp80, and an empty vector control (*EV*) construct. Cells were then stimulated with IL6 for 30 min. EGFR was immunoprecipitated with anti-EGFR monoclonal antibody 108.1 (*IP: EGFR*). Tyrosine-phosphorylated EGFR was detected by immunoblotting with monoclonal anti-phosphotyrosine (*PY*) antibody. The amount of EGFR was analyzed by reprobing the same membrane with anti-EGFR antibody. Cell lysates (*Lysate*) were immunoblotted with anti-p-Stat3 (*p-Stat3*) antibody and reprobed with anti-Stat3 antibody. Phosphorylated p44/42 MAPK (*p-p44/42 MAPK*) was also detected, and the membrane was reprobed with anti-p44/42 MAPK antibody. The *graph* shows analysis of p-p44/42 MAPK levels in the IL6-treated and -untreated cells.

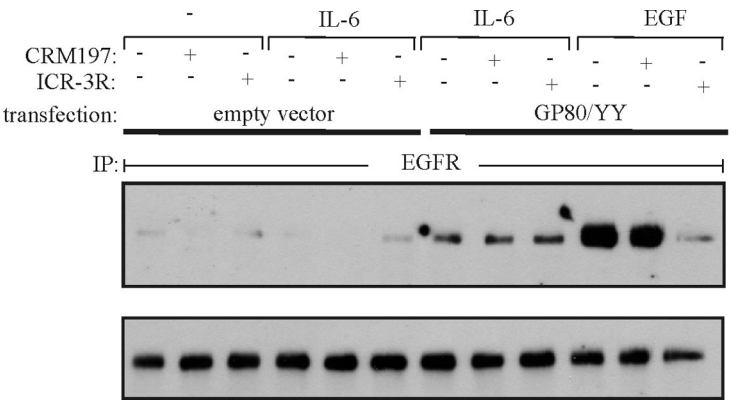

FIG. 8. **EGFR tyrosine phosphorylation upon IL6 stimulation.** COS-7 cells were transiently transfected with cDNAs encoding the mutant gp80-IL6R (*GP80/YY*) (for details see "Experimental Procedures" and the legend to Fig. 7) and an empty vector control plasmid. Cells were stimulated with IL6 or EGF (5 ng/ml) for 20 min followed by an immunoprecipitation of the EGFR with the anti-EGFR monoclonal antibody 108.1 (*IP: EGFR*). Tyrosine-phosphorylated EGFR was detected by immunoblotting with a monoclonal anti-phosphotyrosine (*PY*) antibody. The amount of EGFR was analyzed by reprobing the same membrane with an anti-EGFR antibody.

itors. There is evidence that p44/42 MAPK and p38 MAPK are serine kinases of STATs, and/or they are upstream of a STAT kinase (37). Although the EGFR can activate both Stat3 and p44/42 MAPK, an EGFR inhibitor lowers, but not completely blocks p44/42 MAPK activity, indicating that the p44/42 MAPK was activated also through gp130. These observations suggest that gp130 mediated p44/42 MAPK may serve as a kinase for Stat3 serine phosphorylation. Furthermore, Stat3 activation is partially achieved through the EGFR, which explains why the combination of MAPK and EGFR inhibitors exerts a stronger inhibition on Stat3 activation.

The tyrosine phosphatase SHP2 is important for MAPK activation (38–41). SHP2 phosphorylation was observed in wild-type, gp130Δ/Δ, and Jak2-null mammary tissues suggesting that it could function independently to activate Stat3 during mammary gland involution. This is in agreement with studies on the erythropoietin receptor (EpoR), which lacks all STAT binding sites but retains the membrane proximal region (42). Similar to the results described here the retention of the Jak2 and SHP2 binding sites ensures signaling activity of the EpoR.

Jak1, Jak2, and Tyk2 are reported to activate Stat3 independently. It has been shown that these three kinases play important roles in phosphorylating Stat3 in different cell types. As shown in this study Jak2 is not essential for Stat3 phosphorylation in the mammary epithelial cells. Stat3 can be activated in mammary epithelium by the EGFR, which is not

dependent on Jak2 as the kinase partner. In COS-7 cells, IL6 can trigger a rapid phosphorylation of the EGFR and Stat3 through both wild-type gp130 and a mutant form that lacks Stat3 binding sites. The extent of Stat3 phosphorylation imposed by each individual pathway is not known. However, it is clear from this study that the signaling events through the mutant gp130 are sufficient to complete the process of involution and only loss of the entire protein mimics the impaired remodeling observed in the absence of Stat3. This suggests a possible mechanism of transactivation. A link between Hb-EGF and IL6 has been established in myeloma cells (43) where the inhibition of either Hb-EGF or the EGFR blocked IL6-induced cell growth. However, the mechanism used in mammary epithelium appears to be different since antibodies blocking the EGFR did not abrogate IL6-induced EGFR phosphorylation. In the classical EGFR transactivation ADAM family members of metalloproteases are required for cleavage and release of the transmembrane EGF-like ligand precursors (44–46), which then transactivate the EGFR. While the IL6-induced phosphorylation of the EGFR requires metalloproteases, the mechanism likely does not involve classical EGFR ligands, but rather occurs within the cytoplasm. Notably, a direct interaction between gp130 and the EGFR has been demonstrated (47) and the proximity of the two receptors might permit JAKs to participate in this activation step.

This study emphasizes that the full potential of gp130 receptor-mediated signaling in organogenesis can depend on the transactivation of others receptors and thereby the activation of common downstream transcription factors. This mechanism is operative not only in mammary cells but also in neuronal cells where the competence of cortical progenitors to interpret LIF as an astrocyte-inducing signal is dependent on the presence of Stat3 and the absence of the EGFR results in the inability of these cells to respond to LIF (48). An open question is the nature of the initial stimulus that results in the release of IL6-type cytokines. The current hypothesis is that milk stasis, which develops immediately upon weaning, is the initiating event that triggers a pressure receptor and causes the release of cytokines. These cytokines then broadcast their signals through their distinct receptors, and the common receptor subunit gp130.

Acknowledgments—L. Z. thanks Dr. Keiko Miyoshi for help in tissue transplantation, Dr. Masa Nozawa for his help in animal observation, and all members of the Laboratory of Genetics and Physiology for helpful discussion. L. H. thanks the Alexander von Humboldt Stiftung for generous support while he was on a sabbatical leave as a Humboldt Scholar in Axel Ullrich's laboratory at the Max-Planck-Institute in Martinsried.

REFERENCES

1. Derouet, D., Rousseau, F., Alfonsi, F., Froger, J., Hermann, J., Barbier, F., Perret, D., Diveu, C., Guillet, C., Preisser, L., Dumont, A., Barbado, M., Morel, A., DeLapeyriere, O., Gascan, H., and Chevalier, S. (2004) *Proc. Natl. Acad. Sci. U. S. A.* **101,** 4827–4832
2. Heinrich, P. C., Behrmann, I., Haan, S., Hermanns, H. M., Muller-Newen, G., and Schaper, F. (2003) *Biochem. J.* **374,** 1–20
3. Hibi, M., Murakami, M., Saito, M., Hirano, T., Taga, T., and Kishimoto, T. (1990) *Cell* **63,** 1149–1157
4. Ip, N. Y., Nye, S. H., Boulton, T. G., Davis, S., Taga, T., Li, Y., Birren, S. J., Yasukawa, K., Kishimoto, T., Anderson, D. J., Stahl, N., and Yancopoulos, G. D. (1992) *Cell* **69,** 1121–1132
5. Gearing, D. P., Comeau, M. R., Friend, D. J., Gimpel, S. D., Thut, C. J., McGourty, J., Brasher, K. K., King, J. A., Gillis, S., Mosley, B., Ziegler, S. F., and Cosman, D. (1992) *Science* **255,** 1434–1437
6. Taga, T., and Kishimoto, T. (1997) *Annu. Rev. Immunol.* **15,** 797–819
7. Yoshida, K., Taga, T., Saito, M., Suematsu, S., Kumanogoh, A., Tanaka, T., Fujiwara, H., Hirata, M., Yamagami, T., Nakahata, T., Hirabayashi, T., Yoneda, Y., Tanaka, K., Wang, W. Z., Mori, C., Shiota, K., Yoshida, N., and Kishimoto, T. (1996) *Proc. Natl. Acad. Sci. U. S. A.* **93,** 407–411
8. Ernst, M., and Jenkins, B. J. (2004) *Trends Genet.* **20,** 23–32
9. Ishihara, K., and Hirano, T. (2002) *Biochim. Biophys. Acta* **1592,** 281–296
10. Burdon, T., Smith, A., and Savatier, P. (2002) *Trends Cell Biol.* **12,** 432–438
11. Hennighausen, L., and Robinson, G. W. (2001) *Dev. Cell* **1,** 467–475
12. Zhao, L., Melenhorst, J. J., and Hennighausen, L. (2002) *Mol. Endocrinol.* **16,** 2902–2912
13. Schere-Levy, C., Buggiano, V., Quaglino, A., Gattelli, A., Cirio, M. C., Piazzon, I., Vanzulli, S., and Kordon, E. C. (2003) *Exp. Cell Res.* **282,** 35–47
14. Liu, X., Robinson, G. W., and Hennighausen, L. (1996) *Mol. Endocrinol.* **10,** 1496–1506
15. Chapman, R. S., Lourenco, P. C., Tonner, E., Flint, D. J., Selbert, S., Takeda, K., Akira, S., Clarke, A. R., and Watson, C. J. (1999) *Genes Dev.* **13,** 2604–2616
16. Humphreys, R. C., Bierie, B., Zhao, L., Raz, R., Levy, D., and Hennighausen, L. (2002) *Endocrinology* **143,** 3641–3650
17. Kritikou, E. A., Sharkey, A., Abell, K., Came, P. J., Anderson, E., Clarkson, R. W., and Watson, C. J. (2003) *Development* **130,** 3459–3468
18. Olayioye, M. A., Beuvink, I., Horsch, K., Daly, J. M., and Hynes, N. E. (1999) *J. Biol. Chem.* **274,** 17209–17218
19. Muller, W. J., Arteaga, C. L., Muthuswamy, S. K., Siegel, P. M., Webster, M. A., Cardiff, R. D., Meise, K. S., Li, F., Halter, S. A., and Coffey, R. J. (1996) *Mol. Cell. Biol.* **16,** 5726–5736
20. Ernst, M., Inglese, M., Waring, P., Campbell, I. K., Bao, S., Clay, F. J., Alexander, W. S., Wicks, I. P., Tarlinton, D. M., Novak, U., Heath, J. K., and Dunn, A. R. (2001) *J. Exp. Med.* **194,** 189–203
21. Kopf, M., Baumann, H., Freer, G., Freudenberg, M., Lamers, M., Kishimoto, T., Zinkernagel, R., Bluethmann, H., and Kohler, G. (1994) *Nature* **368,** 339–342
22. Stewart, C. L., Kaspar, P., Brunet, L. J., Bhatt, H., Gadi, I., Kontgen, F., and Abbondanzo, S. J. (1992) *Nature* **359,** 76–79
23. Wagner, K. U., Wall, R. J., St-Onge, L., Gruss, P., Wynshaw-Boris, A., Garrett, L., Li, M., Furth, P. A., and Hennighausen, L. (1997) *Nucleic Acids Res.* **25,** 4323–4330
24. Wagner, K. U., McAllister, K., Ward, T., Davis, B., Wiseman, R., and Hennighausen, L. (2001) *Transgenic Res.* **10,** 545–553
25. Raz, R., Lee, C. K., Cannizzaro, L. A., d'Eustachio, P., and Levy, D. E. (1999) *Proc. Natl. Acad. Sci. U. S. A.* **96,** 2846–2851
26. Shillingford, J. M., Miyoshi, K., Robinson, G. W., Grimm, S. L., Rosen, J. M., Neubauer, H., Pfeffer, K., and Hennighausen, L. (2002) *Mol. Endocrinol.* **16,** 563–570
27. Hilfiker, H., Hattenhauer, O., Traebert, M., Forster, I., Murer, H., and Biber, J. (1998) *Proc. Natl. Acad. Sci. U. S. A.* **95,** 14564–14569
28. Shamay, A., Solinas, S., Pursel, V. G., McKnight, R. A., Alexander, L., Beattie, C., Hennighausen, L., and Wall, R. J. (1991) *J. Anim. Sci.* **69,** 4552–4562
29. Schmitz, J., Dahmen, H., Grimm, C., Gendo, C., Muller-Newen, G., Heinrich, P. C., and Schaper, F. (2000) *J. Immunol.* **164,** 848–854
30. Prenzel, N., Zwick, E., Daub, H., Leserer, M., Abraham, R., Wallasch, C., and Ullrich, A. (1999) *Nature* **402,** 884–888
31. Gerhartz, C., Heesel, B., Sasse, J., Hemmann, U., Landgraf, C., Schneider-Mergener, J., Horn, F., Heinrich, P. C., and Graeve, L. (1996) *J. Biol. Chem.* **271,** 12991–12998
32. Shillingford, J. M., Miyoshi, K., Robinson, G. W., Bierie, B., Cao, Y., Karin, M., and Hennighausen, L. (2003) *J. Histochem. Cytochem.* **51,** 555–566
33. Grandis, J. R., Zeng, Q., and Drenning, S. D. (2000) *Laryngoscope* **110,** 868–874
34. Albanell, J., Rojo, F., and Baselga, J. (2001) *Semin. Oncol.* **28,** 56–66
35. Song, J. I., and Grandis, J. R. (2000) *Oncogene* **19,** 2489–2495
36. Daub, H., Wallasch, C., Lankenau, A., Herrlich, A., and Ullrich, A. (1997) *EMBO J.* **16,** 7032–7044
37. Decker, T., and Kovarik, P. (2000) *Oncogene* **19,** 2628–2637
38. Schiemann, W. P., Bartoe, J. L., and Nathanson, N. M. (1997) *J. Biol. Chem.* **272,** 16631–16636
39. Araki, T., Nawa, H., and Neel, B. G. (2003) *J. Biol. Chem.* **278,** 41677–41684
40. Cunnick, J. M., Meng, S., Ren, Y., Desponts, C., Wang, H. G., Djeu, J. Y., and Wu, J. (2002) *J. Biol. Chem.* **277,** 9498–9504
41. Zhang, S. Q., Yang, W., Kontaridis, M. I., Bivona, T. G., Wen, G., Araki, T., Luo, J., Thompson, J. A., Schraven, B. L., Philips, M. R., and Neel, B. G. (2004) *Mol. Cell* **13,** 341–355
42. Zang, H., Sato, K., Nakajima, H., McKay, C., Ney, P. A., and Ihle, J. N. (2001) *EMBO J.* **20,** 3156–3166
43. Wang, Y. D., De Vos, J., Jourdan, M., Couderc, G., Lu, Z. Y., Rossi, J. F., and Klein, B. (2002) *Oncogene* **21,** 2584–2592
44. Dong, J., Opresko, L. K., Dempsey, P. J., Lauffenburger, D. A., Coffey, R. J., and Wiley, H. S. (1999) *Proc. Natl. Acad. Sci. U. S. A.* **96,** 6235–6240
45. Fischer, O. M., Hart, S., Gschwind, A., and Ullrich, A. (2003) *Biochem. Soc. Trans.* **31,** 1203–1208
46. Schafer, B., Gschwind, A., and Ullrich, A. (2004) *Oncogene* **23,** 991–999
47. Grant, S. L., Hammacher, A., Douglas, A. M., Goss, G. A., Mansfield, R. K., Heath, J. K., and Begley, C. G. (2002) *Oncogene* **21,** 460–474
48. Viti, J., Feathers, A., Phillips, J., and Lillien, L. (2003) *J. Neurosci.* **23,** 3385–3393